SULFIDATION OF

SYNTHETIC BIOTITES

by

Jonathan Lee Tso

Thesis submitted to the Graduate Faculty of the

Virginia Polytechnic Institute and State University

in partial fulfillment of the requirements for the degree of

MASTER OF SCIENCE

in

Geological Sciences

APPROVED:

Dr. M. C. Gilbert, Chairman

Dr. J. R. Craig

Dr. D. A. Hewitt

July, 1977

Blacksburg, Virginia

ACKNOWLEDGEMENTS

The author wishes to thank Dr. M. C. Gilbert, advisor and chairman of the thesis committee for providing encouragement and many fruitful discussions. Dr. J. R. Craig and Dr. D. A. Hewitt provided much help in the laboratory, and in their suggestions in review of this manuscript.

The author also wishes to acknowledge the help of and in the preparation of the manuscript and for his support.

This research was partially funded by NSF grant DES72-01587 AO2.

TABLE OF CONTENTS

INTRODUCTION

The alteration of host rock silicates by sulfur-bearing fluids during formation of sulfide ore bodies has been recognized as yielding important clues in unraveling the history of these bodies. The petrogenesis of ore masses, however, is often obscured by the fact that sulfide mineral assemblages commonly do not reflect their peak conditions of metamorphism due to relatively rapid re-equilibration at lower temperatures (Yund and Hall, 1969). The use of the pyrite-pyrrhotite geothermometer is an example of this (Yund and Hall, 1969). As a result, determinations of the nature of sulfur-rich vapors based on compositions of pyrrhotite are frequently not in agreement with evidence based on silicate mineral assemblages. Hence, there has been much attention focused on silicates and oxides in the gangue and wall-rocks which presumably do not re-equilibrate as rapidly as sulfides and still indicate, to a greater extent, the conditions of metamorphism.

One geochemical pattern previously recognized is the systematic decrease in Fe/(Fe + Mg) in iron-magnesium silicates as one moves from the wall-rock toward the ore-body, with magnesium-rich compositions found in the gangue within the ore-body. Such an effect for biotites has been documented by Staten (1976), Fullagar *et al.* (1967) and Harvey (1975). Meaningful interpretation of this pattern as an indication of silicate interaction with a sulfur-rich fluid in the ore zone, requires that the following criteria be met: 1) equilibrium has been approached or reached, 2) the bulk chemistry of the silicate portion inside and outside the ore-body was originally the same or may be estimated if not the same, and 3) iron was not preferentially added to or taken from the

system or that the degrees of exchange can be calculated. A study by Bachinski (1976), however, did not show such a pattern for chlorites in Newfoundland. This demonstrates that the preceding criteria must be considered very carefully. However, in all these cases, Fe-Mg silicates are apparently responsive to the fugacity of sulfur during metamorphism or alteration.

Experimental studies of sulfide-silicate reactions have been done to only a limited extent. Kullerud and Yoder (1963, 1964) mixed various ferro-magnesian silicates with sulfur and found, when starting with intermediate compositions, more magnesium-rich silicates and sulfides in addition to various breakdown products at the conclusion of their runs. Whereas these earlier experiments were of a qualitative nature, Naldrett and Brown (1967) produced the first reversed experiments on sulfide-silicate reactions, equilibrating pyrrhotite and enstatite-ferrosilite solid solutions using evacuated silica glass tubes. This method was extended by Clark and Naldrett (1972) in a study of Fe-Ni partitioning between olivine and sulfide and by Rajamani (1976) for Co-Ni partitioning in orthopyroxene and sulfide. Hammarbäck and Lindqvist (1972) produced a set of hydrothermal experiments on biotites by using an oxide mix plus sulfur in gold tubes. While their results show a general trend of more sulfur-rich pyrrhotites coexisting with more magnesium-rich biotites, they did not demonstrate equilibrium. Popp et al. (1977), in experiments with coexisting pyrrhotite-orthoamphibole solid solutions, modified previous techniques so that reversibility in hydrothermal runs could be demonstrated. This method was used here in an attempt to equilibrate pyrrhotite and biotites along the join

phlogopite-annite.

Ideally, the following reaction takes place for biotites:

$$KFe_3AlSi_3O_{10}(OH)_2 + 3/2\ S_2 \rightleftarrows KAlSi_3O_8 + 3FeS + H_2O + 3/2\ O_2 \quad (1)$$

(Fe-component in biotite) (Vapor) (K-spar) (Pyrrhotite) (Vapor)

If magnetite is also present, then the reaction

$$KFe_3AlSi_3O_{10}(OH)_2 + 1/2\ O_2 \rightleftarrows Fe_3O_4 + KAlSi_3O_8 + H_2O \quad (2)$$

(Fe-component in biotite) (Vapor) (Magnetite) (K-spar) (Vapor)

must also occur. Combining reactions (1) and (2) yields the important equilibrium relation between magnetite and pyrrhotite,

$$Fe_3O_4 + 3/2\ S_2 \rightleftarrows 3FeS + 2\ O_2 \quad (3)$$

In reactions (1) and (2), the iron component in biotite breaks down when it reacts with the vapor to leave behind a biotite enriched in magnesium. Concurrently, reaction (3) is a "sliding scale" buffer where the non-stoichiometric composition of pyrrhotite defines f_{S_2} and therefore f_{O_2} if pure magnetite is present. The relationship between pyrrhotite composition and f_{S_2} has been experimentally determined by Toulmin and Barton (1964).

During the course of metamorphism (and these experiments) a fourth reaction may take place:

$$FeS_2 \rightleftarrows FeS + 1/2\ S_2 \quad (4)$$

(Pyrite) (Pyrrhotite) (Vapor)

EXPERIMENTAL METHODS

The experiments employed a "triple-layer" arrangement in a double gold capsule as depicted in figure 1. The inner capsule (0.04" outside radius) contained pure synthetic starting material + 4-5 mg. distilled H_2O and was divided into the following layers: 1) Fe-rich biotite + pyrite, 2) magnetite + sanidine, 3) Mg-rich biotite + stoichiometric FeS (troilite) $\pm$ magnetite $\pm$ sanidine. By convention, this study will label layer 1 as the top, layer 2 as the middle and layer 3 as the bottom. The constituents of the individual layers were mixed for several minutes by hand in an agate mortar and carefully packed into the tube. The tube was welded shut and the vacant portion at the top of the capsule was flattened and bent as an indicator of the orientation of the layers.

This capsule was, in turn, placed in a larger gold capsule (0.10" outside radius) and surrounded by magnetite + quartz + 30 mg. distilled H_2O. The purpose of the outer capsule and its "buffer" is twofold: 1) to help physically isolate the inner capsule; 2) to help provide limitations on the f_{O_2} of the charge with the upper limit being the magnetite-hematite buffer curve and the lower limit being the fayalite-magnetite-quartz buffer curve. No hematite or fayalite was ever found in the outer capsule after a run.

The capsules were run in standard cold-seal hydrothermal apparatus with temperatures measured by bare-wire chromel-alumel thermocouples calibrated at one atmosphere against the melting point of NaCl (800.5°C) and CsCl (646°C). The accuracy of measurement is estimated at $\pm$ 5°C. Pressures were measured by factory calibrated Heise Bourdon-tube

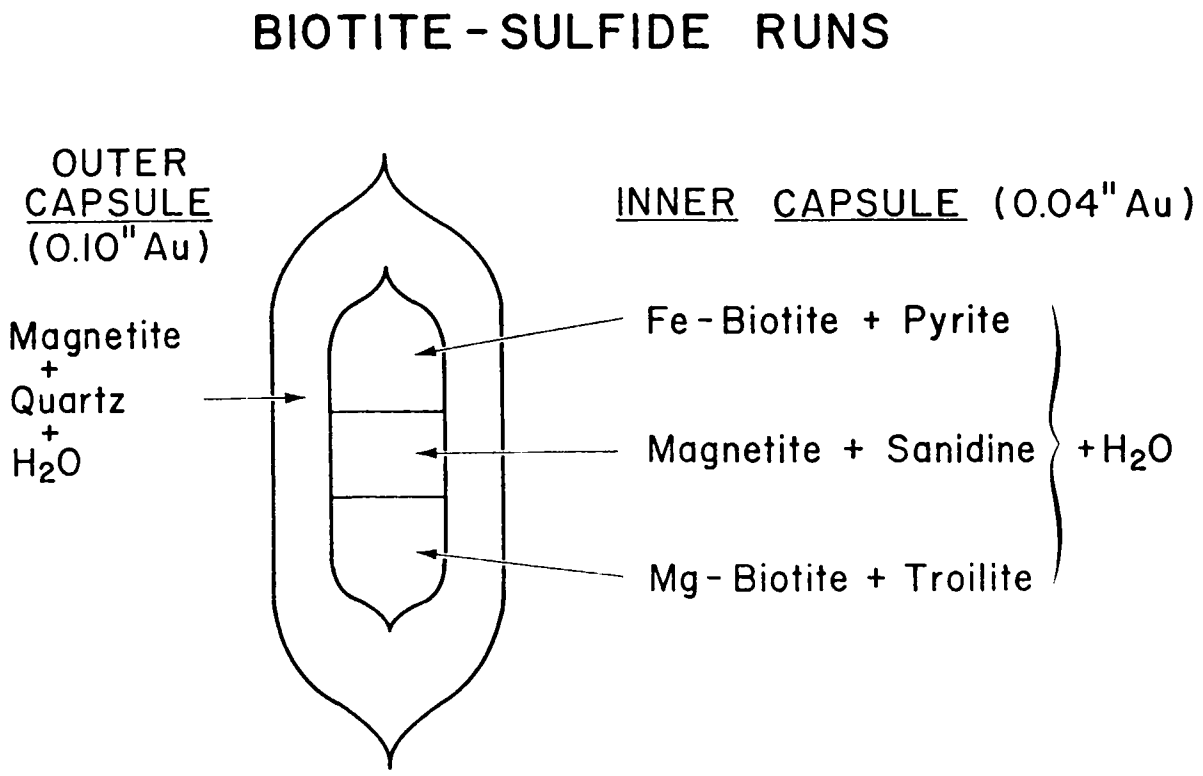

Figure 1. Schematic of capsule arrangement showing the three layers, outer capsule and their constituents.

gauges which are assumed accurate to $\pm$ 50 bars. Typical run times were two weeks.

Runs were quenched by blowing a stream of air over the vessels for one minute and then immersing them in cold water. On opening the inner capsule, a stronger odor of H_2S, when compared to the outer, signified the effective sealing of the capsule. An examination of the charge showed that the three layers were easily distinguished by their color. The layers were then separated and saved for analysis.

A run was considered to be a "bracket" if there was a single, homogeneous composition of pyrrhotite present throughout the capsule, and the composition of the biotite in one layer is observed to change from Fe-rich to more Mg-rich and the biotite in the other layer is observed to change from Mg-rich to more Fe-rich. Analysis of the run products will be discussed later.

SYNTHESIS OF STARTING MATERIAL

Biotite

The biotites used in this study lie compositionally along the join annite-phlogopite. Both end members plus two intermediate compositions ($KMg_2Fe_1AlSi_3O_{10}(OH)_2$ and $KMg_1Fe_2AlSi_3O_{10}(OH)_2$) were synthesized from oxide-glass mixes prepared as follows:

A glass of the composition $K_2Si_4O_9$ was made from the following: K_2CO_3 prepared from $KHCO_3$ (Fisher lot 712479) and SiO_2 glass (Corning lump cullet #7940) treated with nitric acid. The glass was prepared by the method described in Schairer and Bowen (1955) and was found to be optically homogeneous after several crushing and melting cycles. It has an index of refraction of $1.495 \pm .001$.

γ - alumina was produced by heating $AlCl_3 \cdot 6H_2O$ (Fisher lot 711038) in a silica glass boat at 700°C until a constant weight was achieved. The material was then placed at 900°C for 2 hours. No alumino-silicates were observed.

MgO (Materials Research Corp. job no. 30635) was dried at 1000°C for 1-2 hours.

Fe-sponge (Johnson Mathey & Co.) was checked for oxygen content by weighing a few grams of it in a silica glass boat, reducing it with an H_2 flow at 500°C for 30 hours and reweighing it. An oxygen content correction factor was then calculated and applied to the Fe-sponge used in the mix.

These materials were combined with more SiO_2 glass to give the proper compositions and were mixed in a mechanical agate mortar under alcohol for about 4 hours until judged homogeneous.

The iron-bearing mixes plus distilled H_2O were loaded into $Ag_{70}Pd_{30}$ tubes and run at various temperatures and 1000 bars methane with graphite filler-rods. It was found necessary to regrind and reload the charges once to produce runs of ≥ 95% biotite. Phlogopite was synthesized in gold tubes (0.10" outside radius) in standard hydrothermal apparatus at 700 to 800°C, 2000 bars for 7 days. The charge consisted of > 98% biotite.

Portions of the Fe-bearing biotites were annealed in Pt tubes at the Ni-NiO buffer for one week for comparison with the physical property data given by Wones (1963), using his regression curves for the relations between the physical properties and Fe/(Fe + Mg) of biotite. The data obtained in this study, given in table 1, show good agreement between the observed d(060/$\bar{3}$31) and the d-value calculated from the curves of Wones. It was found that a best fit between measured and calculated values was obtained if the "quadratic" rather than the "linear" expression of Wones was used. The comparison between the measured n_γ and calculated n_γ also shows agreement well within the error of measurement. Measurements were aided by use of a wavelength interference filter employing a "single variation" technique. Measurements of a number of grains show an essentially homogeneous composition of samples.

Table 2 is a list of unit-cell dimensions assuming a 1M polytype although it was found that the measured powder reflections agreed well with either a 1M or 3T polytype. The 1M polytype was used in order to be consistent with values reported by Eugster and Wones (1962), Wones (1963), and Hewitt and Wones (1975). Several low intensity biotite peaks, however, were found that did not agree with the 1M or 3T structure.

Table 1

Comparison of annealled biotites (NNO, 600°C, 2000 bars) and predicted physical properties and compositions from Wones (1963)

Composition of starting mix Fe/(Fe + Mg)	Measured d(060/$\bar{3}$31)	Predicted d(060/$\bar{3}$31)	Predicted Fe/(Fe + Mg) from measured d(060/$\bar{3}$31)
*0.0	1.5351(5)	1.5348(4)	0.012
	[a]1.5349(6)		0.004
	[b]**1.5346(2)		-0.008
0.33	1.5429(5)	1.5427(4)	0.338
0.67	1.5503(5)	1.5498(4)	0.696
1.00	1.5572(5)	1.5556(4)	1.103
	[c]1.5568		1.077
	[d]1.5550(10)		0.963

[a]Wones (1963)

[b]Hewitt and Wones (1975

[c]Rutherford (1973)

[d]Eugster and Wones (1962)

*not annealled at 600° C, NNO

**calculated d($\bar{3}$31) from regression equation

***calculated n_γ from regression equation

Table 1 (cont.)

Composition of starting mix Fe/(Fe + Mg)	Measured n_γ	Predicted n_γ	Predicted Fe/(Fe + Mg) from measured n_γ
*0.0	1.583 ± .002	1.581(3)	0.022
	[a]1.581 ± .001		0.002
	[b]***1.583(1)		0.022
0.33	1.617 ± .002	1.616(3)	0.339
0.67	1.657 ± .002	1.657(3)	0.674
1.00	1.696 ± .002	1.700(3)	0.971
	[d]1.697 ± .002		0.978

Table 2

Unit cell dimensions for annealed biotites (600°C, 2000 bars, NNO)

Fe/(Fe + Mg)	a(Å)	b(Å)	c(Å)	β	V(Å^3)
*0.0	5.319(2)	9.193(3)	10.313(3)	99.90(3)	496.7(2)
	[a]5.326(6)	9.210(9)	10.311(9)	100.17(13)	497.77
	[b]5.317(1)	9.203(2)	10.310(2)	99.92(1)	496.9(1)
	[b]5.318(2)	9.206(5)	10.308(2)	99.83(2)	497.2(3)
0.33	5.349(2)	9.245(4)	10.311(3)	99.95(3)	502.2(2)
0.67	5.371(2)	9.297(3)	10.304(3)	99.95(3)	506.7(2)
1.00	5.395(2)	9.340(3)	10.300(3)	100.00(2)	511.1(2)
	[c]5.381(10)	9.330(6)	10.285(20)	99.93(25)	--

[a]Wones (1963)

[b]Hewitt and Wones (1975)

[c]Eugster and Wones (1962)

*not annealed at NNO

Following the discussion of Hewitt and Wones (1975), these peaks indicate the presence of a small portion of $2M_1$ mica. The presumed small free energy difference between these polytypes is not expected to significantly affect the results of the experiments.

K-feldspar

K-feldspar was produced by mixing together $K_2Si_4O_9$ glass, SiO_2 glass, and γ-alumina, loading into gold capsules + H_2O and running at 750°C, 1000 bars for 3 days. Results were 99% feldspar. Unit cell dimensions obtained from powder X-ray methods are: a = 8.602(1)Å, b = 11.302(2)Å, c = 7.179(1)Å and β = 116.02(1)°. The powder pattern agrees with that given by Borg and Smith (1969) for high sanidine.

Quartz

The quartz used was Fisher (lot 711367) silica (140 mesh) which was treated in HCl and then sulfuric acid.

Pyrite and Troilite

The starting sulfides were synthesized from ASARCO sulfur chips (99.999% pure) and iron sponge (Johnson Mathey & Co., reduced at 900°C with an H_2 flow in evacuated silica glass tubes.

Magnetite

The magnetite used was ferric-ferrous oxide black (Fisher lot 783353). An x-ray and reflected light study showed only magnetite present. This material was not annealled.

ANALYSIS OF RUN PRODUCTS

Run products were identified and characterized by: 1) transmitted and reflected light studies and 2) X-ray diffraction, using a Norelco or Picker powder diffractometer. For peak position determinations, a CaF_2 internal standard (a=5.4632(14)Å) was used.

Biotites

Two methods of determination of composition were used. Firstly, measurements of d-values of the composite $\bar{3}31$-060 peak, in conjunction with the regression equations of Wones (1963), were used as a preliminary means for compositional measurements. As the equations from Wones are applicable only to biotites at the oxygen fugacity defined at various solid buffers, and with the oxygen fugacity of the sulfidation runs intermediate between that defined by the solid buffers, a method of interpolation was found to be necessary. In figure 2, lines of constant d-value are plotted as a function of log f_{O_2} and Fe/(Fe + Mg) for synthetic biotites at 600°C and 2000 bars. These d-values are plotted for compositions of Fe/(Fe + Mg) = 0.0, 0.33, 0.67 and 1.0, normalized against the NNO buffer, using the regression equations of Wones (1963). Values of f_{O_2} for NNO and MH are taken from Huebner (1971) and the value for FMQ is from Hewitt (Personal communication, 1977). Since all of the sulfidation experiments fall between NNO and MH, and the lines of constant d-value on figure 2 approximate a straight line between FMQ and MH, a linear interpolation between NNO and MH was considered valid.

Secondly, the n_γ of biotite was measured, again using the regression curves of Wones (1963) and interpolating between curves when necessary.

Figure 2. Lines of constant d-spacing on a log f_{O_2} - Fe/(Fe + Mg) diagram.

Dots represent locations calculated from the regression equations of Wones (1963), normalized at NNO. The crosses (X) are locations of the annealled biotites from this study calculated from the equations of Wones (1963).

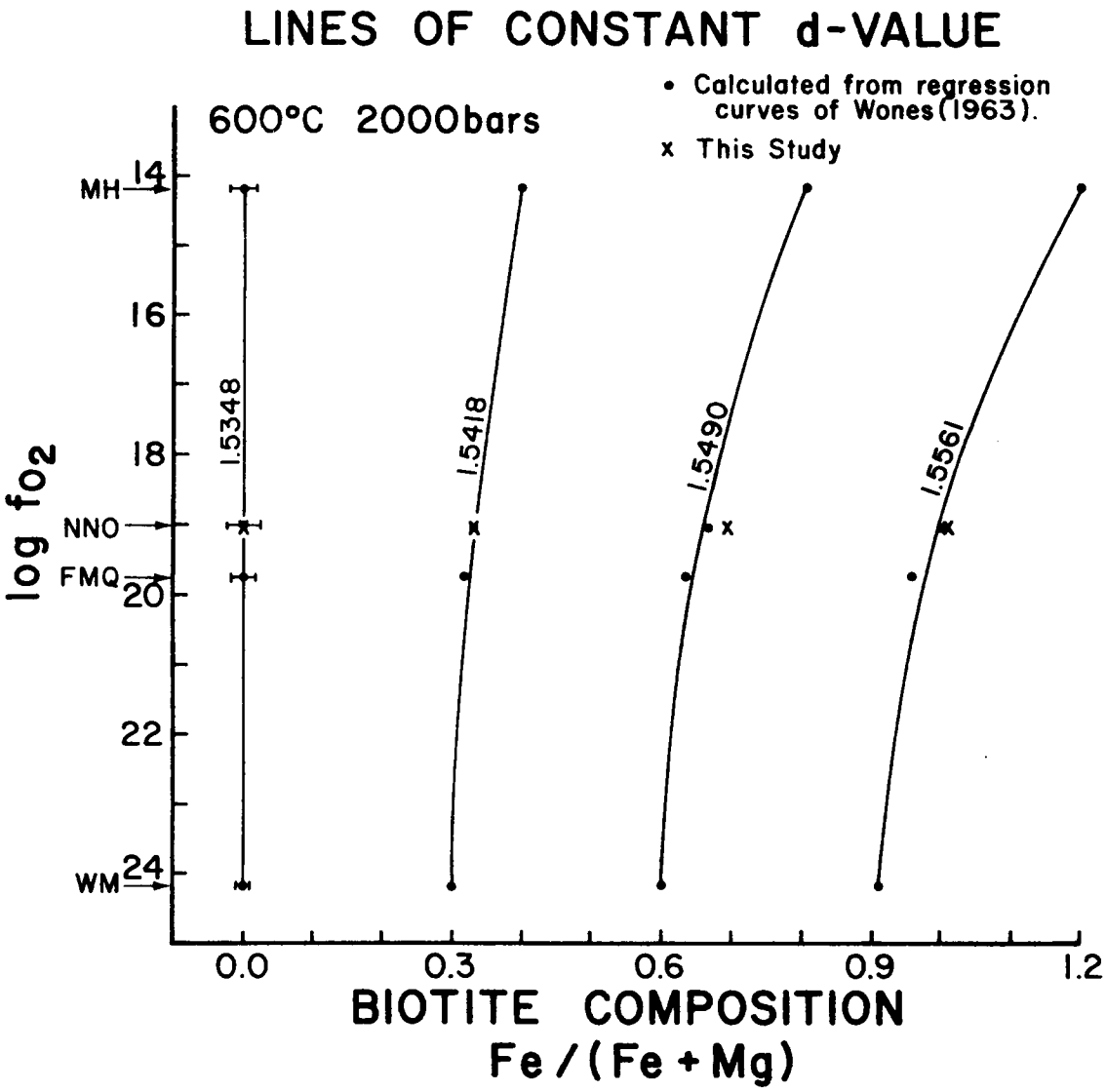
LINES OF CONSTANT d-VALUE
600°C 2000bars
• Calculated from regression curves of Wones(1963).
x This Study
MH
NNO
FMQ
WM
14
16
18
20
22
24
log fO2
1.5348
1.5418
1.5490
1.5561
0.0
0.3
0.6
0.9
1.2
BIOTITE COMPOSITION
Fe/(Fe+Mg)

In oils, the biotites were seen to be in platelets ranging in size from less than 1 μm to 10 μm in length, showing pleochroism and a suggestion of zoning in the coarsest grains from the layer with the originally more Fe-rich biotite. Figure 3 shows the result of the measurement of a number of grains (4-8 μm) from a single typical reversal experiment. A scatter of compositions was observed. However, the edge of the reversal bracket is considered to lie between the most Mg-rich biotite in the top layer and the most Fe-rich biotite in the other layer. This criterion is only applied to the runs in which each layer started with a single composition of biotite. The reversal bracket determined is consistent with that determined by the X-ray powder method but carries a smaller uncertainty.

Finally, the assumption was made that the biotites do not differ in composition, at termination of bracketing runs, from those along the phlogopite-annite join. No significant deviations in composition off the join has ever been detected. For natural biotites, Banks (1973) has observed up to 345 ppm. of sulfur in some form in biotite. Such concentrations, if present in our biotites, are assumed not to affect significantly the physical or chemical properties. No descrepancies between optical and X-ray determinations from Wones (1963) that would indicate an aluminous biotite (Hewitt and Wones, 1975) were observed for the equilibrium runs.

Pyrrhotite

In reflected light, pyrrhotite is seen to occur as equant, untwinned grains up to 50 μm across, commonly containing blebs of magnetite or rarely pyrite. Compositions were determined by means of the d(102) peak,

Figure 3. Comparison of optical and X-ray measurements for run #30, 700°C, 2000 b.

The arrow on the optical measurement diagram is the location of the bracket; the midpoint between the most magnesium-rich biotite observed from the top and the most iron-rich biotite from the bottom.

OPTICAL AND X-RAY MEASUREMENTS OF BIOTITE COMPOSITION FOR A SINGLE RUN

RUN#30, 700°C, 2000b, $N_{po} = 0.947$

HISTOGRAM OF OPTICAL MEASUREMENT

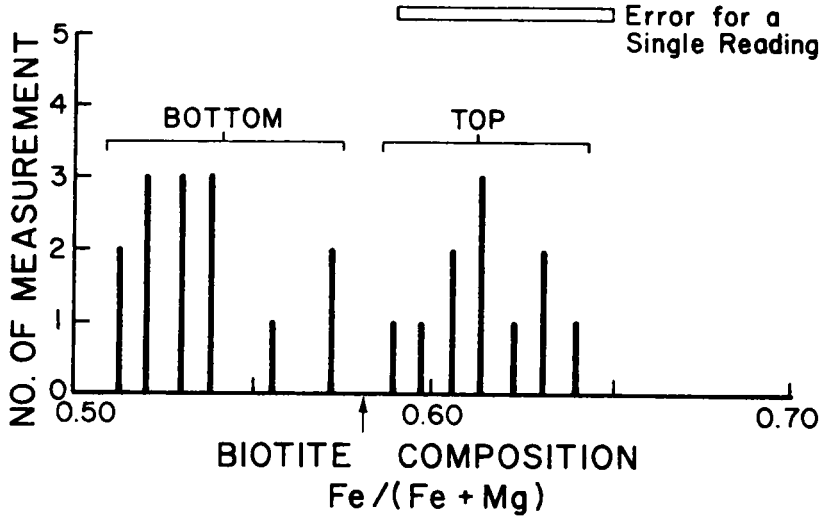

X-RAY MEASUREMENT

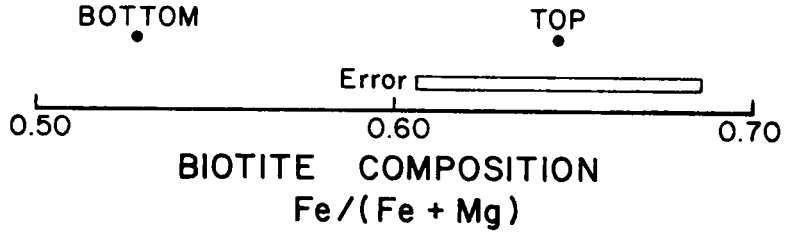

using the relation between d-value and composition given by Yund and Hall (1969). Only runs in which the compositions were within an N value of $\pm$ .002, the experimental uncertainty, were used. Occasionally, the peak coincided with one for magnetite for those compositions close to troilite, or were too weak to measure accurately. In these cases, the runs were not used for equilibrium determinations.

A number of runs were found to contain pyrite in the top and bottom. Pyrrhotite compositions in these runs frequently showed significant differences between the layers. These pyrrhotites were assumed not to reflect their equilibrium compositions and that some, if not all, of the pyrite was exsolved on quenching. As a result, these runs were not used in defining "brackets."

Pyrite

Pyrite was found only in the most sulfur-rich runs and normally was accompanied by Al-rich magnetite and langbeinite. In reflected light, it appears as 1) discrete grains up to 30 μm, or 2) as smaller blebs in or adjacent to magnetite or pyrrhotite. Pyrite is more commonly found in the layer in which it was added, but its presence in the bottom signifies that not all the pyrite can be considered as unreacted starting material.

Textural evidence was generally inconclusive as to the mode of origin. All of the pyrite observed in 800° runs, above its melting point, is clearly a result of quenching. However, it is possible that the pyrite could have formed from both the quenching of a liquid or from the exsolution of pyrrhotite as it re-equilibrated. The appearance of the charge in these 800°C runs was distinctive in that it was granular

(grain sizes of approximately 0.2 mm) rather than the more normal compact powder.

Magnetite

As observed in polished section, magnetite had two modes of occurrences. In runs at relatively low f_{S_2}, it appeared similar to the starting material: extremely fine grained (i.e. less than several microns). In such cases, magnetite was difficult to determine optically but could be clearly identified by X-ray methods. Detection of magnetite was difficult in runs in which no middle layer, or no magnetite, was used in the capsule.

The second mode of occurrence was observed at higher f_{S_2}, especially at 800°C. The magnetite is coarser (up to 30 μm), occurring as blebs or euhedral grains in pyrrhotite or pyrite and also as discrete grains. Under close observation, these magnetites sometimes exhibited weak reddish internal reflections. Partial microprobe analyses (table 3) were carried out for Fe, Mg and Al to check for possible solid solution. Although up to 15 weight percent magnesioferrite component is known from magnetites in pyrite-pyrrhotite bearing magnetite ores from Sweden (Annersten, 1969), the analyses showed smaller amounts of Mg but enrichment in Al. The occurrence of pyrite in these runs, causing difficulties in demonstrating pyrrhotite equilibration, as previously described, prevented the use of these experiments as "brackets."

K-feldspar

K-feldspar is either irregularly shaped or blocky (especially in the middle layer) with the average size being 5-10 μm. Qualitative microprobe data of a few random samples show negligible iron content. Kalsilite and leucite were not detected.

Table 3 Microprobe analyses of magnetites

Run no.	29,mid	36,mid	36,top	*22,mid	*22,mid	*37,mid	*37,mid
T^{o} C	700	800	800	800	800	800	800
Al_2O_3	0.00	0.12	0.35	7.23	5.00	2.07	1.91
FeO	87.66	88.63	88.32	82.77	82.96	85.00	86.20
MgO	0.27	0.55	0.55	0.70	0.64	0.87	0.73
Total	87.94	89.30	89.23	90.71	88.61	87.94	88.84

all Fe was calculated as Fe^{2+}

*pyrite was a run product.

Langbeinite ($K_2Mg_2(SO_4)_3$)

This sulfate is found in high f_{S_2} conditions and usually was observed along with aluminous magnetite, pyrite, quartz, and pyroxene, if detectable. Because of its extremely fine grained manner, it is difficult to identify optically but is seen clearly in the X-ray powder pattern. As a result of difficulties in demonstrating pyrrhotite equilibration in all these runs, experiments with langbeinite were not used as equilibrium runs.

As a test, it was synthesized at 700°C and 2000 bars by taking reagent K_2SO_4 and $Mg(SO_4)_2 \cdot 7H_2O$, dissolving in H_2O, drying the precipitate, grinding and running in a gold tube for one day. The capsule gave off water upon opening with a strong odor of H_2S. After drying, an optical and X-ray check showed 90% langbeinite with the rest being various other sulfates.

Quartz

Quartz was observed in only one run and occurs with pyroxene and langbeinite. In this particular run, biotite broke down completely and no sanidine was detected. It was observed to average about 10 μm in size although one grain was estimated to be 50 μm.

Pyroxene

In the run that shows quartz, minor amounts of pyroxene of undetermined composition is present. Optically, it occurs in roundish grains in sizes of less than 2 μm. X-ray peaks are consistent with that of enstatite. No fayalite was ever observed.

DETERMINATION OF THE OXYGEN FUGACITY

It has been demonstrated by numerous authors (for example Eugster and Wones, 1962; Wones, 1963) that the physical properties of biotites vary according to the oxidizing conditions of the experiment. This is due to an "oxy-biotite" component in which, theoretically, Fe^{3+} substitutes for Fe^{2+} in the octahedral layer, with the loss of a proton. Therefore, since the oxygen fugacity was not externally buffered or directly measured, it was necessary to calculate it from equation (3):

$$Fe_3O_4 + 3/2\ S_2 \rightleftarrows 3\ FeS + 2\ O_2. \qquad (3)$$

Such an approach has been taken by Popp et al. (1977) and their data plus new determinations done during this study have been used to experimentally locate the magnetite-pyrrhotite curve in log f_{O_2} - log f_{S_2} space.

Experiments at 600°, 750° and 800°C were performed using the triple-layer method with fayalite + quartz + magnetite + pyrite in the one end of the capsule, fayalite + quartz + magnetite + troilite in the other end, and fayalite + quartz + magnetite in the middle layer and outer capsule. After runs of one week, fayalite + magnetite + quartz + pyrrhotite was present throughout the capsule, with the composition of pyrrhotite appearing everywhere homogeneous. Presence of this assemblage defines a point on the magnetite-pyrrhotite curve where the composition of pyrrhotite defines f_{S_2}, and the assemblage fayalite-quartz-magnetite defines f_{O_2}.

Using the equation for the relationship between d(102) and N of pyrrhotite given by Yund and Hall (1969) and the equation for N, log f_{S_2}, and log a_{FeS}^{Po} from Toulmin and Barton (1964), corrected to

2000 bars, the data in table 4 were generated. Oxygen fugacity was determined by means of the equation of Hewitt (Personal communication, 1977). The data of Popp et al. (1977) have been modified to be in accord with the above relations. Once the experimental point has been located, K may be calculated and, assuming constant K, the slope of the line can be determined from the equation:

$$\log K = 2 \log f_{O_2} + \log a^{Po}_{FeS} - 3/2 \log f_{S_2}, \qquad (5)$$

for a given f_{S_2}. A comparison of the curve location at 700°C, 2000 bars for that reported by Popp et al. (1977), and that calculated using thermodynamic data (see Popp et al. (1977) for the method of calculation) with the location based on the methods used in this study is shown in figure 4. It is seen that the present location is closer to the calculated curve than that of Popp et al., but well within the limits of error established for these curves. The slight curvature in the line is due to the changing activity of pyrrhotite.

A plot of all the curves determined is shown in figure 5. In actual practice, for a sulfidation run, the pyrrhotite compositions were determined by way of the d(102)-value, with the log f_{S_2} calculated as previously described. Using the appropriate curve, log f_{O_2} was determined. Then, the composition of biotite was corrected to f_{O_2} by a linear interpolation of the measured physical property between the regression curves given in Wones (1963).

Table 4

FAYALITE-MAGNETITE-QUARTZ-PYRRHOTITE EQUILIBRIA

2000 bars

T°C	Pyrrhotite Composition (N±0.002)			$\log f_{S_2}$	$\log f_{O_2}$
	Upper	Lower	Average	(±0.35)	(±0.20)
600	.9608	.9604	.9606	-5.39	-19.76
650*	.9621	.9601	.9611	-4.71	-18.20
675*	.9617	.9617	.9617	-4.41	-17.49
700*	.9650	.9642	.9646	-4.37	-16.81
725*	.9661	.9636	.9649	-4.08	-16.16
750	.9629	.9625	.9627	-3.56	-15.55
800	.9629	.9638	.9634	-3.06	-14.41

*Determined by Popp *et al*. (1977)

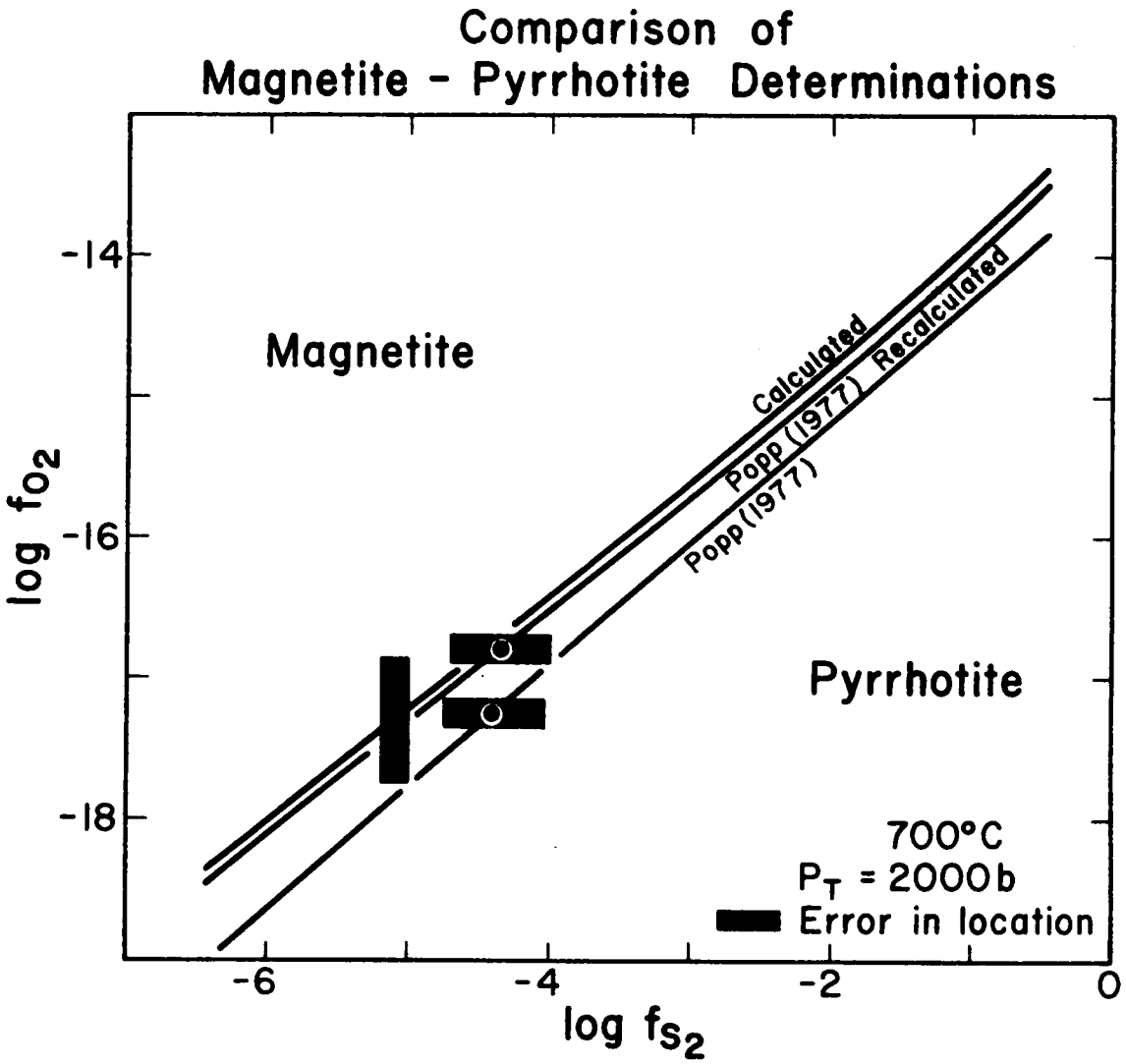

Figure 4. Comparison of locations for the Magnetite-pyrrhotite curve, 700°C, 2000 b. Dots represent location of the determined equilibrium assemblage fayalite-quartz-magnetite-pyrrhotite.

Calculated - from thermodynamic data
Popp (1977) - position given by Popp et al. (1977)
Popp (1977) - recalculated - a redetermining of the data of Popp et al. (1977) using the equation for log f_{O_2} from Hewitt (Personal communication, 1977) and the d-value vs. composition equation given by Yund and Hall (1969).

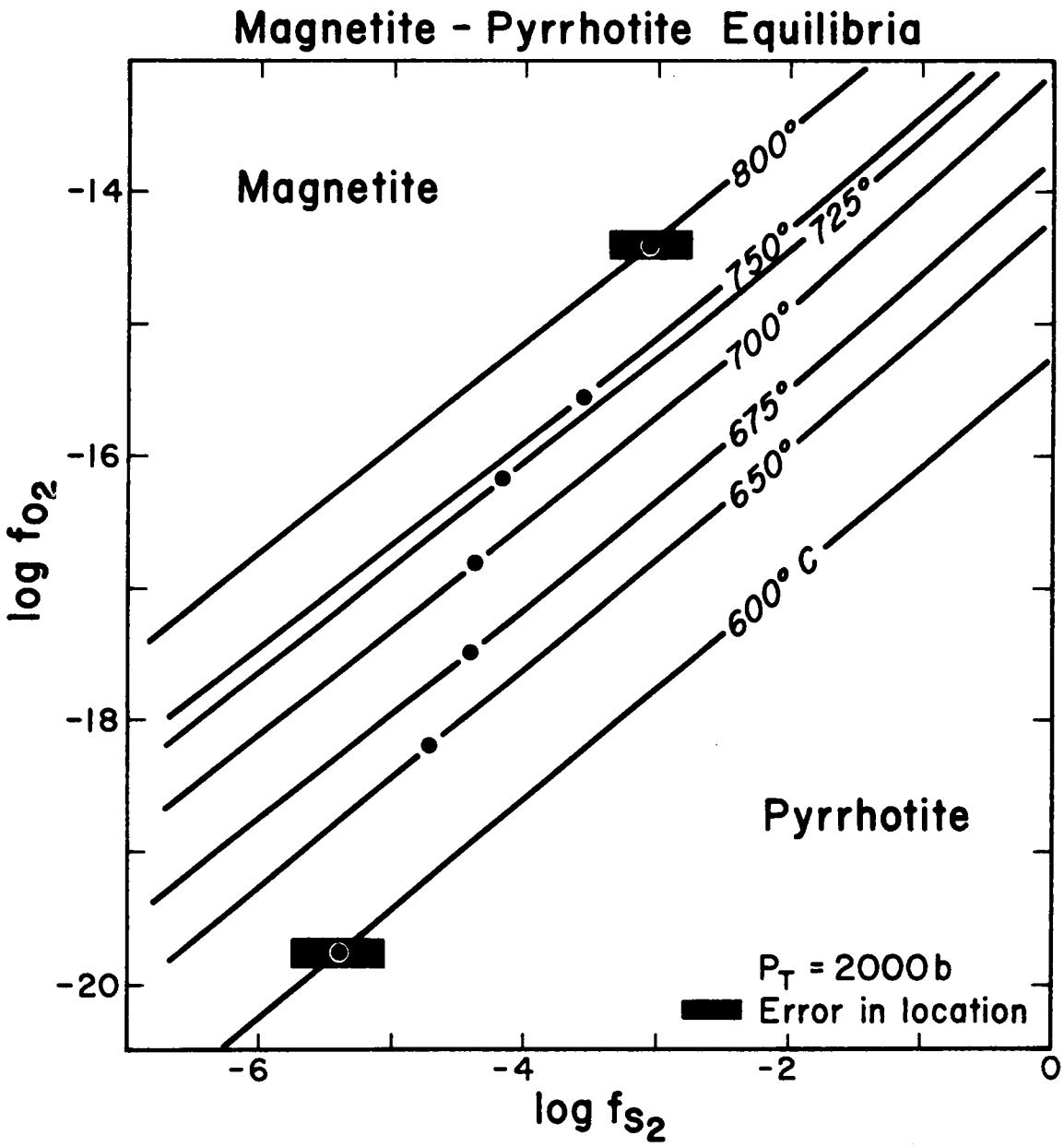

Figure 5. A plot of all experimental determinations for the magnetite-pyrrhotite curve on a log f_{O_2} - log f_{S_2} plot.

DISCUSSION OF RESULTS

Table 5 lists the results of all the experiments attempted on the sulfidation of biotites. Of the experiments, the ones considered to determine "tie-lines" meet the following criteria: 1) pyrrhotite compositions (N) between the top and bottom must be within $\pm$ .002, 2) the final composition of biotite is intermediate between the starting compositions of the top and bottom, and 3) magnetite is present.

Runs may be categorized into several types: 1) compositions of the biotites shifted in the same direction, either to the more Fe-rich or the more Mg-rich direction, 2) compositions of one layer moved from Fe-rich to more Mg-rich while the compositions of the other layer moved from the Mg-rich to the more Fe-rich or 3) no change was detected on one layer but change was detected on the other layer. In the first group of experiments in table 5, the annite and phlogopite end-members were used at each end. Results show that in the layer starting with annite, biotite breaks down completely to sanidine + magnetite + pyrrhotite while the other layer shows an increase in annite content of biotite.

Preliminary compositions based on X-ray determinations, as previously described, were useful as a guide to the trends of the experiments but they proved to be misleading in cases where a mixture of two biotites of different compositions were used as starting material in the individual layers. X-ray analyses showed essentially an average of compositions, but when checking optically determined compositions, a wide range of Fe/(Fe + Mg) values was found. Appreciable overlap of compositions from top to bottom was observed, probably due to sluggish-

Table 5 Compositional determinations of run products.

Run No.	Time	Pyrrhotite Composition (N) Final Upper	Final Lower	Biotite Composition (Fe/Fe + Mg) Starting Upper	Starting Lower	Final Upper	Final Lower	X-ray
				650°				
2	14d 14h	.9601	.9618	1.00	0.0	-	.095	
[a] 6	47d 16h	.9427	.9416	1.00	0.0	-	.314	
				700°				
1	3d 20h	.9524	.9539	1.00	0.0	-	.174	
3	14d 14h	.9267	.9254	1.00	0.0	-	.218	
4	14d 14h	.9274	.9284	1.00	0.0	-	.217	
[a] 5	14d 14h	.9401	.9419	1.00	0.0	-	.226	
7	14d 14h	.9415	.9405	1.00	0.0	-	.258	
8	57d 11h	.9318	.9327	1.00	0.0	-	.339	
[b] 9	57d 11h	.9279	weak	1.00	0.0	-	.090	
				600°				
[b,c] 10	14d 18h	.9379	.9258	.67	.33	.146	.235	
13	14d 20h	.9236	.9261	.67+0.0	.33+0.0	.310	.262	

Table 5 (cont.)

Run no.	Time	Pyrrhotite Composition (N) Final Upper	Final Lower	Biotite Composition (Fe/Fe + Mg) X-ray Starting Upper	Starting Lower	Final Upper	Final Lower
[c,d]15	13d 23h	.9210	.9160	.67	.33	.442	.398
18	14d 0h	e	e	.67+0.0	.33+0.0	[h].281	[h].302
[b]21	20d 21h	.9229	weak	.67	.33	.432	.365
[b]23	22d 19h	.9221	.9168	.33	0.0	.341	.114
31	14d 23h	.9451	.9466	.67	.33	.517	.442
32	14d 22h	.9280	.9286	.67	.33	.558	.490
				700°			
[b,c,d]11	14d 15h	.9200	.9206	.67	.33	.297	.257
12	15d 20h	.9232	.9451	.67+0.0	.33+0.0	.324	.234
14	14d 15h	.9395	.9457	.67+0.0	.33+0.0	.413	.471
[c,d]16	14d 7h	.9371	.9371	.67	.33	.492	.474
19	13d 20h	.9307	.9356	.67+0.0	.33+0.0	.442	.417
[b]24	32d 19h	.9186	weak	.33	0.0	.273	.180
26	15d 18h	.9223	.9263	.33	0.0	.401	.376

Table 5 (cont.)

Run no.	Time	Pyrrhotite Composition (N) Final Upper	Final Lower	Biotite Composition (Fe/Fe + Mg) X-ray Starting Upper	Starting Lower	Final Upper	Final Lower
28	15d 2h	.9282	.9303	.67	.33	.491(.516)	.415(.475)
[g]29	16d 3h	.9438	.9452	.67	.33	.537(.570)	.492(.511)
[g]30	17d 9h	.9472	.9466	.67	.33	.645(.589)	.528(.572)
33	14d 23h	.9373	.9360	.67	.33	.534(.530)	.503(.530)
[g]34	14d 21h	.9518	.9499	.67	.33	.629(.593)	.588(.576)
				800°			
[b,c,f]20	16d 19h	.9269	.9277	.67	.33	-	-
[b]22	17d 18h	.9287	.9212	.67	.33	weak	weak
[b]25	19d 24h	.9163	.9183	.33	0.0	.370	.340
[b,g]35	8d 8h	.9258	.9178	.67	.33	.423	.388
[g]36	8d 0h	.9239	.9274	.67	.33	.504	.425
[b,g]37	9d 0h	weak	weak	.33	0.0	weak	weak
[g]38	8d 21h	.9415	.9428	.33	0.0	.518	.506

Table 5 (cont.)

[a]no outer layer

[b]pyrite present after quenching

[c]no middle layer

[d]magnetite not present

[e]interference with mt peak

[f]quartz and pyroxene were run products

[g]wustite in middle layer

[h]assuming f_{O_2} of NNO

( )edge of optical bracket

ness of biotite equilibration, and hence, no bracket could be assigned.

Several points of technique require additional discussion. In order to control roughly the f_{S_2}, varying amounts of sulfide, and occasionally mixtures of pyrite + troilite in the top were used. This method was found to be fairly successful, but better control was achieved by mixing in synthetic wustite in the middle layer in place of magnetite. This resulted in a lower value of f_{S_2}. In all cases, magnetite + pyrrhotite was the assemblage found at the end of such runs. The mixing in of hematite should allow higher f_{S_2} conditions to occur, but in our experiments, this was not found necessary.

Five well-reversed tie-lines at 700°C and 2000 bars are plotted in figure 6. The trend is similar to that found by Popp et al. (1977), with increasing magnesium enrichment in the silicate as a function of increasing sulfur content of pyrrhotite. The equilibrium biotite composition is placed mid-way between the most Mg-rich biotite from the top and the most Fe-rich biotite from the bottom, as measured optically. The pyrrhotite composition is an average of the X-ray determined compositions found at each end of the capsule. Since the pyrrhotite composition is related to f_{S_2}, the relationship of Toulmin and Barton (1964), corrected to pressure, yields the f_{S_2} for a given biotite composition.

The system may be represented on a log f_{O_2} - log f_{S_2} plot (Holland, 1959 and Frose, 1971) at 700°C and 2000 bars as shown in figure 7, using the experimentally located magnetite-pyrrhotite curve assuming stoichiometric magnetite and K-spar. The biotite compositional fields are represented as contours representing reactions (1) and (2), intersecting on the magnetite-pyrrhotite curve, the location of the five

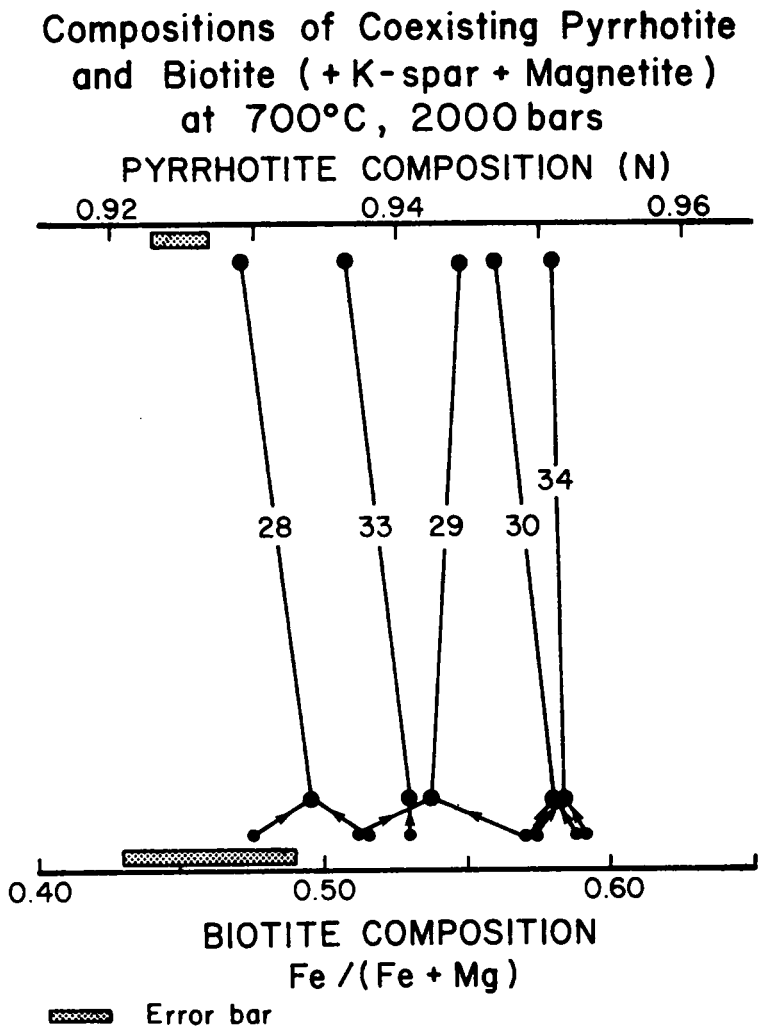

Figure 6. Biotite-pyrrhotite equilibria.

The biotite compositions are the averages between the most Mg-rich biotite optically observed in the top and the most Fe-rich composition of the bottom. Arrows indicate "bracketing" compositions of the top and bottom. Pyrrhotite compositions are average N values between top and bottom. Run numbers are listed on the tie-lines.

Figure 7. Biotite stability on the log f_{O_2} - log f_{S_2} plot at 700°, 2000 b. Positions of the buffers MH, NNO and FMQ are indicated by arrows on the log f_{O_2} axis. Numbers in parentheses are the compositions of biotite with magnetite + sanidine taken from Wones and Eugster (1965). Dashed line is the extrapolated curve of a biotite of Fe/(Fe + Mg) of 0.39. Numbers in brackets represent calculated Fe/(Fe + Mg) from the solution model of Wones and Eugster (1965).

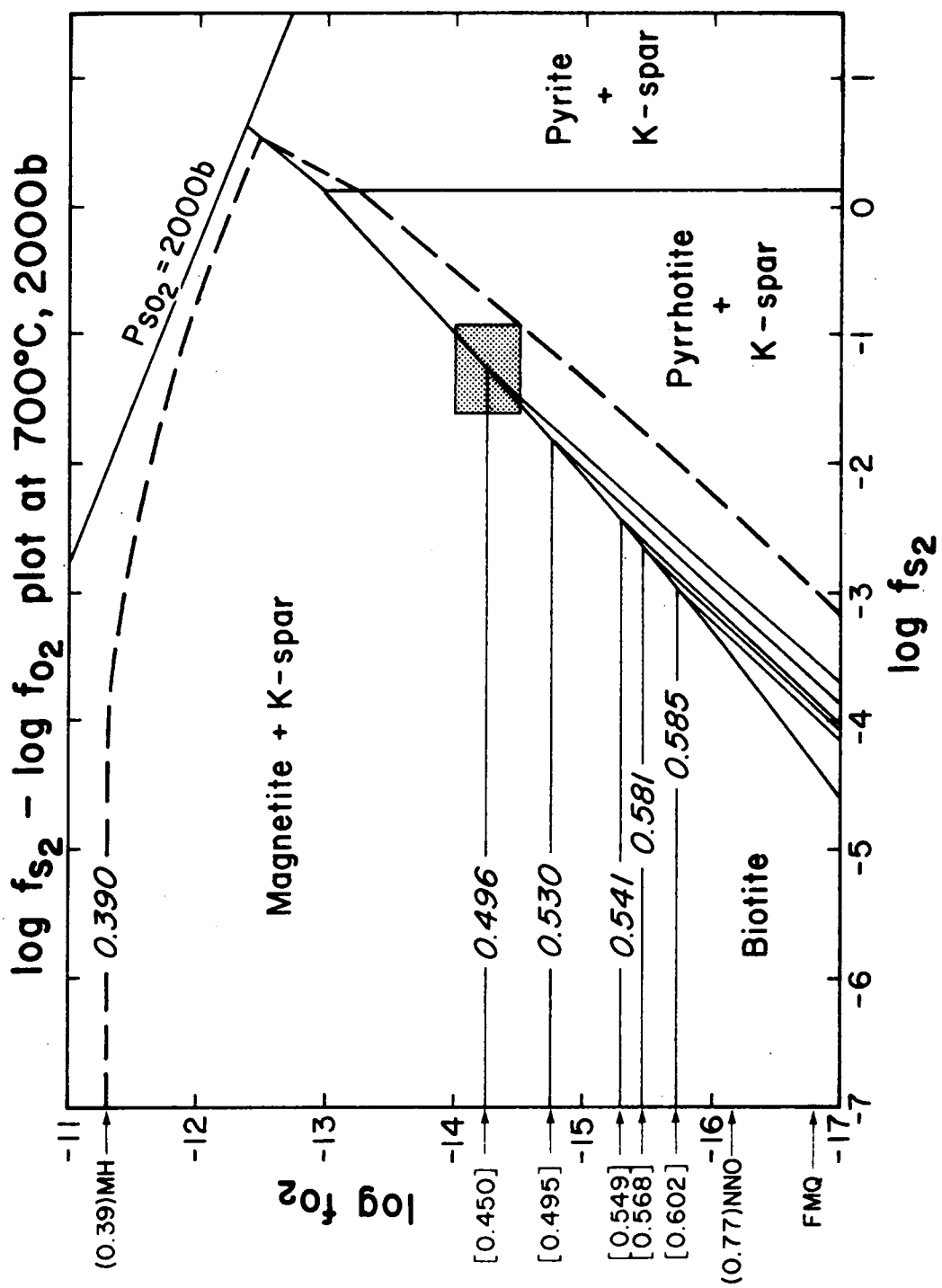
log f_{S_2} – log f_{O_2} plot at 700°C, 2000b
P_{SO_2} = 2000b
0.390
Magnetite + K-spar
Pyrite + K-spar
Pyrrhotite + K-spar
Biotite
0.496
0.530
0.541
0.581
0.585
log f_{O_2}
log f_{S_2}
(0.39)MH
[0.450]
[0.495]
[0.549]
[0.568]
[0.602]
(0.77)NNO
FMQ
-11
-12
-13
-14
-15
-16
-17
0
-1
-2
-3
-4
-5
-6
-7

experimental points. The curves for reaction (2), as will be shown later, can be extrapolated horizontally from the experimental points to the log f_{O_2} axis, essentially the sulfur-free system. There, one can make a comparison between this study and one made by Wones and Eugster (1965) in which the stability of biotite (reaction 2) was determined as a function of temperature, pressures of 1035 and 2070 bars, using solid buffers. Their experimental compositions are in parentheses next to the arrows signifying the position of the solid buffers.

As will be discussed in the next section, log f_{H_2} can be calculated for all of the equilibrium experiments. This allows a comparison of the experimentally determined compositions of biotite with predicted compositions based on the solution model of Wones and Eugster (1965). The compositions obtained in this manner are in brackets on figure 7 and are well within the experimental error of this study.

COMPOSITION OF THE VAPOR

In an H-O-S vapor, the value for f_{H_2} can be calculated using the method of Eugster and Skippen (1967), assuming ideal mixing, given a specified f_{O_2} and f_{S_2}. From this, one may calculate the fugacities of any of the vapor species. This calculation has been done by Popp et al. (1977) and their vapor phase calculations are identical to these. Table 6 is a list of sources for activity coefficients and equilibrium constants. The species for which calculations were made were H_2, H_2O, SO_2, SO, H_2S, HS and H_2SO_4. Such calculations have been used by Bachinski (1976) in natural systems. Figure 8 is a series of maps calculated at 600, 700, and 800°C showing lines of constant f_{H_2}. From any point on these maps, one can easily estimate the fugacity of any species anywhere on the diagram by use of the proper equations.

Focusing on figure 8b, at 700°C, several things occur. There is a region at relatively high log f_{O_2} - log f_{S_2} where the calculated partial pressure of SO_2 exceeds the total pressure of 2000 bars. This area is not, therefore, physically realizable. Note also that the assemblage magnetite + hematite + pyrite is in this area at 700°.

Reaction (2) may be rewritten:

$$KFe_3AlSi_3O_{10}(OH)_2 \rightleftarrows Fe_3O_4 + KAlSi_3O_8 + H_2 \qquad (6)$$

As a result, for a constant composition and pure magnetite and K-spar:

$$\log K = \log f_{H_2} - \log a_{Fe}^{Biot} \qquad (7)$$

Therefore, assuming constant K and a given biotite composition, the curve for reaction (6) should parallel the log f_{H_2} contours on the log f_{O_2} - log f_{S_2} plot, essentially straight horizontal lines over most of

Table 6

List of references for the calculation of H-O-S vapor.

Value	Reference
Equilibrium constants	JANAF Tables (1971)
Fugacity coefficients	
H_2	Shaw and Wones (1974)
H_2O	Burnham et al. (1969)
H_2S	Ryzhenko and Volkov (1971)
SO_2	Hougen et al. (1964)

All other fugacity coefficients were assumed equal to unity.

Figure 8a. Lines of constant log f_{H_2} on a log f_{O_2} - log f_{S_2} plot for 600°C. Dashed lines represent oxide-sulfide equilibria. Abbreviations are as follows: mt - magnetite; po - pyrrhotite; and py - pyrite. Numbers in parentheses represent location of the experimentally determined compositions of intermediate biotite by Wones and Eugster (1965) at various solid buffers. The numbers in brackets represent the location of annite by Rutherford (1973).

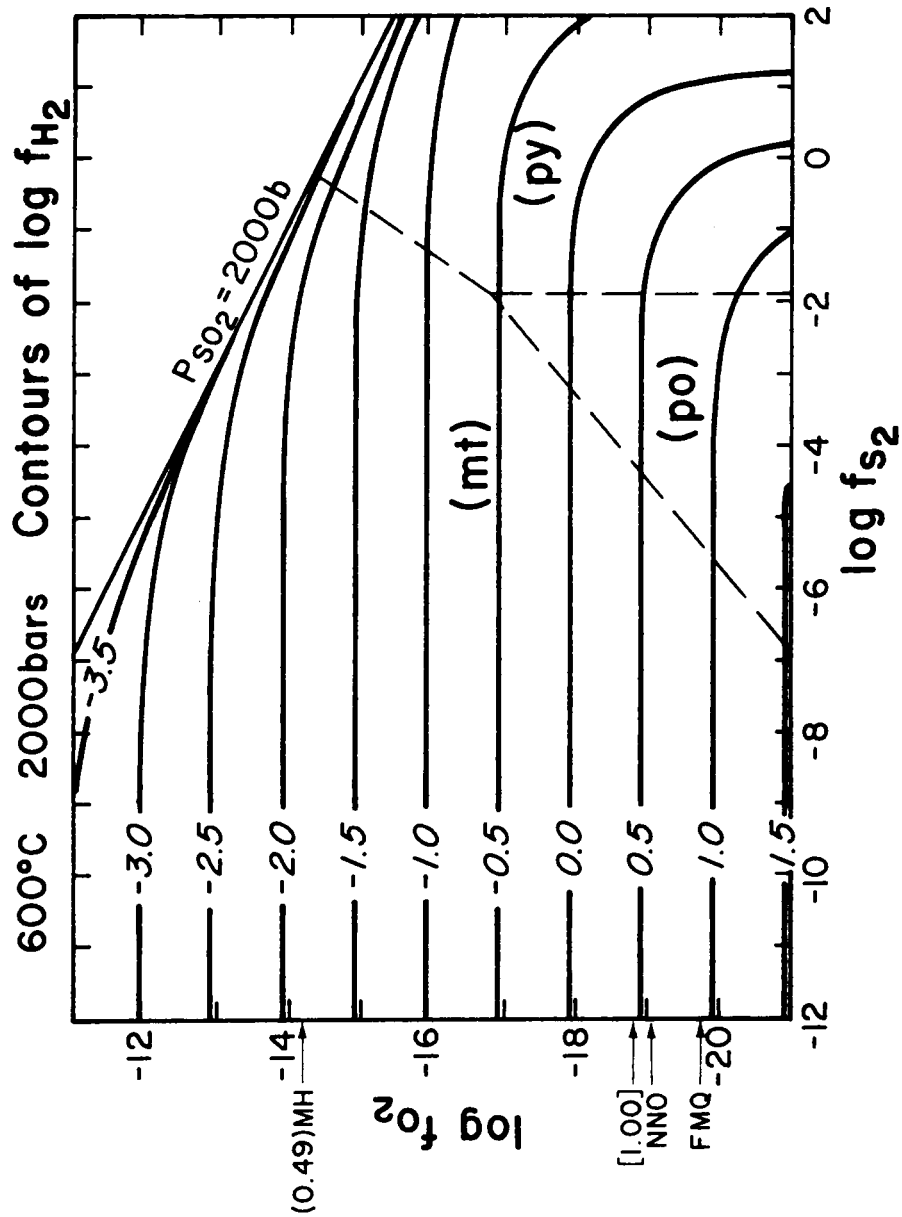
600°C 2000bars Contours of log f_{H_2}
P_{SO_2}=2000b
-3.5
-3.0
-2.5
-2.0
-1.5
-1.0
-0.5
0.0
0.5
1.0
1.5
(mt)
(py)
(po)
log f_{O_2}
log f_{S_2}
-12
-14
-16
-18
-20
2
0
-2
-4
-6
-8
-10
-12
(0.49)MH
[1.00]
NNO
FMQ

Figure 8a

Figure 8b. Lines of constant log f_{H_2} on a log f_{O_2} - log f_{S_2} plot at 700°C. Abbreviations are the same as that used for figure 8a.

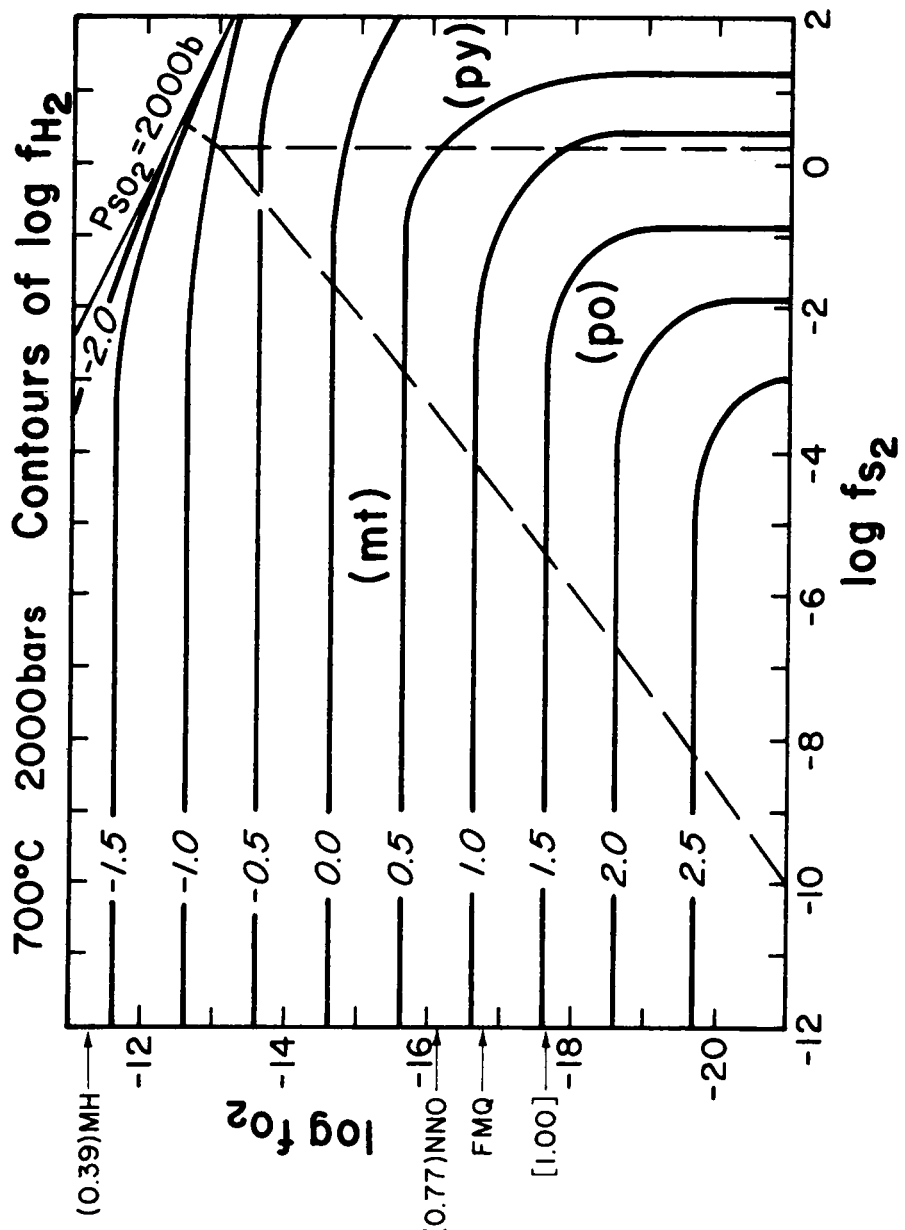
700°C 2000bars Contours of log f_{H_2}
P_{SO_2}=2000b
-2.0
-1.5
-1.0
-0.5
0.0
0.5
1.0
1.5
2.0
2.5
(py)
(po)
(mt)
log f_{S_2}
log f_{O_2}
(0.39)MH
(0.77)NNO
FMQ
[1.00]

Figure 8b

Figure 8c. Lines of constant log f_{H_2} on a log f_{O_2} - log f_{S_2} plot at 800°C. Abbreviations are the same as that used for figure 8a.

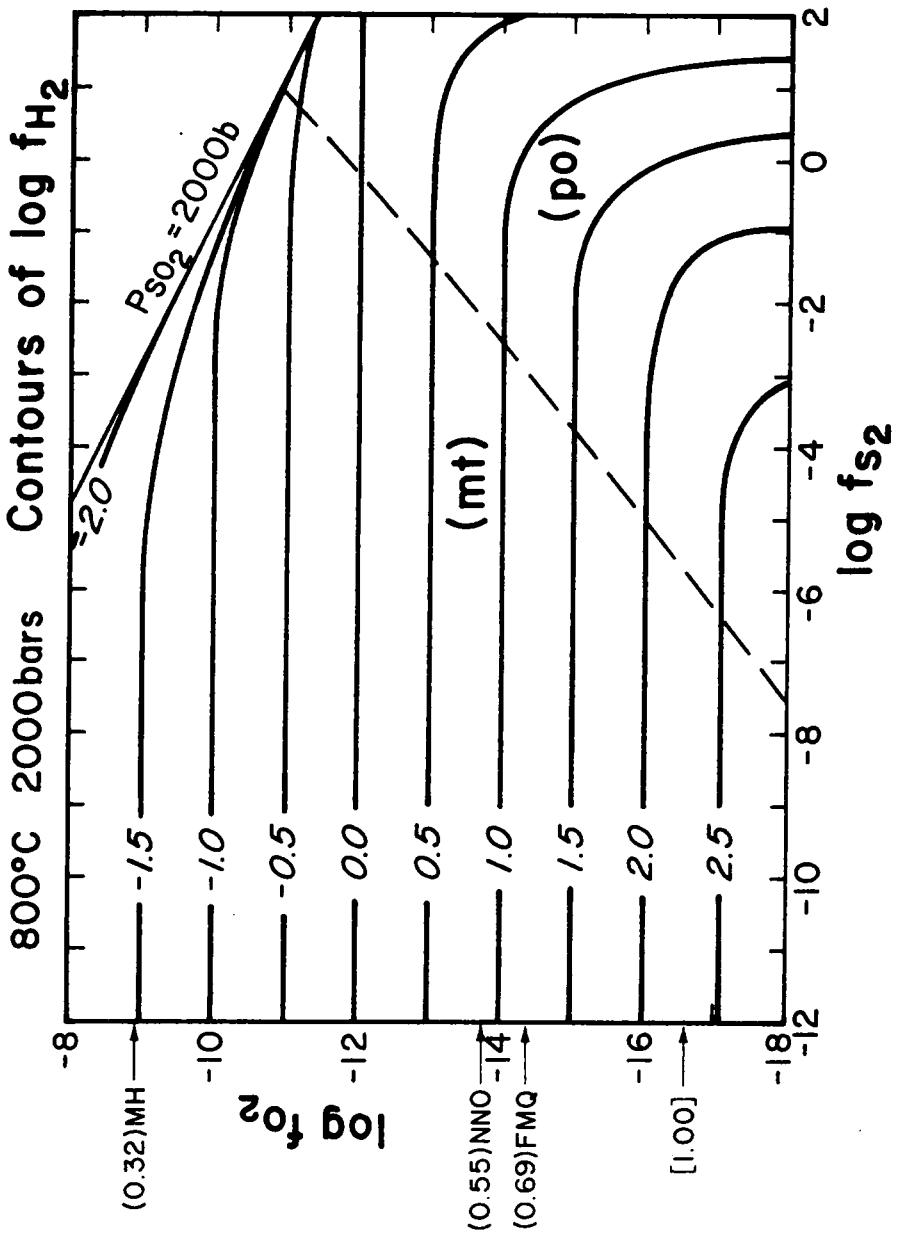
800°C 2000bars Contours of log f_{H_2}
P_{SO_2} = 2000b
-2.0
-1.5
-1.0
-0.5
0.0
0.5
1.0
1.5
2.0
2.5
(mt)
(po)
log f_{O_2}
log f_{S_2}
(0.32)MH
(0.55)NNO
(0.69)FMQ
[1.00]
-8
-10
-12
-14
-16
-18
2
0
-2
-4
-6
-8
-10
-12

Figure 8c

the f_{O_2} dominated portion of the diagram. Extrapolation from the experimental points to the f_{O_2} side should therefore be possible. However, a magnesium-rich biotite of Fe/(Fe + Mg) of 0.39 stable at the magnetite-hematite buffer (Wones and Eugster, 1965) would not extrapolate linearly, but would be limited by the existence of the SO_2 "impossible" area. Its curve (dashed line on figure 7) would bend "down" toward the more sulfur-rich portion of the diagram.

The fact that the results of these experiments show agreement with the experimental data and solution model of Wones and Eugster (1965) is an independent indication that approach to equilibrium has been achieved.

Conversely, incompatability with the preceding criterion indicates a non-attainment of equilibria. A test of the data of Hammarbäck and Lindqvist (1972) given in Table 7 shows the following: assuming, for the sake of simplicity, that their experiments at 575°C and 1600 atm. can plot as a fair approximation on figure 8a at 600°C, 2000 bars, it is seen that a number of their runs do not show sufficiently high Fe/(Fe + Mg) for the reported log f_{S_2} to satisfy the determinations of Wones and Eugster (1965). For example, two runs are reported as having pure phlogopite (with magnetite + sanidine + pyrrhotite), compositions that should show an oxide-sulfide assemblage of magnetite (with possible hematite) and pyrite, rather than magnetite-pyrrhotite. In addition, the crossing of tie lines is an indication of non-equilibrium. It should, of course, be noted that Hammarbäck and Lindqvist did not claim that their experiments represented equilibrium.

Table 7

Data at 575°C and 1600 atm from Hammarbäck and Lindqvist (1972)

Duration (Days)	X(of annite) Fe/(Fe + Mg)	log f_{S_2}
16	0.580	-6.4
16	0.355	-6.1
16	0.100	-5.5
16	0	-5.2
16	0	-4.7
23	0.370	-6.0
23	0.390	-5.8
23	0.215	-5.9
23	0.290	-6.1
23	0.180	-5.7

GEOLOGICAL APPLICATIONS

Biotites are common in a wide variety of rocks and are, as a result, important minerals in gangue associated with sulfide ores. Unfortunately, there is a dearth of chemical data on biotites in many assemblages involving coexisting sulfides to which the experimental data reported here could be applied. However, whenever coexisting sulfides and biotites have been investigated, interaction during crystallization appears to have occurred. This is true whether the assemblages are in ore deposits, regional metamorphic terranes, or igneous rocks.

In igneous rocks, for example, Putnam (1972) describes biotite in granites from the Rocky Hill and Lights Creek Stocks, Sierra Nevada, California, in which the copper content of the sulfides shows an inverse relationship with the copper content of Fe-Mg silicates. The effect of migrating fluids of changing compositions in the Chino Porphyry Copper Deposit has been discussed by Jacobs and Parry (1975). These authors noted that low pH, high Fe/Mg fluids yielded higher Fe-biotites and that high pH, low Fe/Mg fluids yielded higher Mg-biotites. Beane (1974), compiling data on altered biotites from a number of porphyry copper environments, has proposed a geothermometer based on the observation that altered biotites tend to show a lower Fe/Mg and a lower Fe^{3+}/Fe^{2+} than unaltered biotites.

In metamorphic terranes, Guidotti (1970) has shown notable decreases in Fe/(Fe + Mg) in biotites from N. W. Maine with only the addition of 3 modal percent sulfide. Robinson and Tracy (1977) can demonstrate correlations between types of sulfide-silicate-oxide assemblages and Fe-content of biotite in pelitic rocks of Central Massachusetts. Staten

(1976) has shown systematic changes in biotite composition from the Great Gossan Lead, S.W. Virginia as a function of distance from an ore toward pelitic-psammatic schists. Here the Fe/(Fe + Mg) ratio is 0.264 in the ore zone; 0.404, five feet into the country rock; and 0.477, seven feet or more into the country rock, indicating a relatively narrow alteration around the ore body. In these studies, however, the absence of magnetite + K-spar prevents the direct application of the experimental results.

A number of localities having the assemblage biotite-sulfide-magnetite are reported in the literature, but quantitative studies of biotite composition from these areas are rarely reported. Moh et al. (1964) reports such an assemblage at Ducktown, Tennessee and a study by Harvey (1975), from the same location, qualitatively indicates a higher content of Mg relative to Fe in biotites closer to the ore body. At Ore Knob, North Carolina, Fullagar et al. (1977) have related an increase in the index of refraction of biotite to distance as one moves up to hundreds of feet away from the ore body.

Caution should be exercised before applying the experimental results to natural systems. Unless an oxygen fugacity-indicating mineral assemblage is present, estimation of location on a log f_{O_2} - log f_{S_2} plot is uncertain. The importance of noting carefully the oxide and sulfide phases becomes clear. The presence of graphite, for example, indicating a vapor containing species such as CO_2, CH_4, etc., leads to further complications. These more complex fluids would likely have reduced f_{H_2} relative to the C-free system, and therefore reduced f_{H_2O}, limiting the biotite stability field over that found in the H-O-S system.

The presence of various solid solutions in biotites (and also in magnetite) in more complex chemical systems could further modify results. In this study, it is reasonably assumed that biotite compositions do not differ very much from those along the annite-phlogopite join, and that if such slight deviations exist, it would negligibly effect the physical properties of the biotites. In nature, many biotites contain significant amounts of Al^{IV} and Al^{VI} substitution for Fe^{VI} and Si^{IV}. Studies by Rutherford (1973) suggest that such a substitution would result in an increase of biotite stability in the same manner as the substitution of Mg^{VI} for Fe^{VI} (Wones and Eugster, 1965). Nevertheless, it is hoped that a simple approximation allowing comparison of the natural samples with the experimental results obtained from this study can be used once the biotite compositions have been determined. The effect of substitutions of Cu, Ni, Co, etc. on sulfide-biotite relations has been neglected.

Although the experimental data are inconclusive with regards to the effect of temperature on the compositional tie-lines between pyrrhotite and biotite, the study by Popp et al. (1977) indicates that the temperature effect on the sulfidation reaction introduces no appreciable change in the sulfide-silicate compositions relative to one another. Therefore, in order to use the silicate composition to estimate sulfur fugacity, the temperature must be determined by an independent method.

In summary, it is vitally important that a careful physical and chemical examination of all the phases present in an assemblage be made. Additional experimental studies of sulfide-silicate reactions are obviously needed to further clarify such complex questions as the effect of

various cationic substitutions in both silicates and sulfides and the effect of a more complex vapor composition on the reactions. But, experimental data, combined with careful field and analytical studies, promises to eventually result in the determination of adequate models for the petrogenesis of many sulfide ore bodies.

REFERENCES

Annersten, H. (1969) Magnetites from a sulphide bearing iron ore formation in Sweden. Mineral. Deposita (Berl.), 4, 234-240.

Bachinski, D. J. (1976) Metamorphism of cupriferous iron sulfide deposits, Notre Dame Bay, Newfoundland. Econ. Geol., 71, 443-452.

Banks, N. G. (1973) Biotite as a source of some sulfur in porphyry copper deposits. Econ. Geol., 68, 697-708.

Beane, R. E. (1974) Biotite stability in the porphyry copper environment. Econ. Geol., 69, 241-256.

Borg, I. Y. and K. K. Smith (1969) Calculated X-ray powder patterns for silicate minerals. Geol. Soc. Am. Mem. 122, 896 p.

Burnham, C. W., J. R. Hollaway and N. F. Davis (1969) Thermodynamic properties of water to 1000°C and 10,000 bars. Geol. Soc. Am. Special Pap. 132, 96 p.

Clark, T. And A. J. Naldrett (1972) The distribuiton of Fe and Ni between synthetic olivine and sulfide at 900°C. Econ. Geol. 67, 939-952.

Eugster, H. P. and G. Skippen (1967) Igneous and metamorphic reactions involving gas equilibria. In, P. H. Abelson, Ed., Researches in Geochemistry, Vol. 2. John Wiley and Sons, New York, 663 p.

_____ and D. R. Wones (1962) Stability relations of the ferruginous biotite, annite. J. Petrol., 3, 82-125.

Frose, E. (1971) The graphical representation of sulfide-silicate phase equilibria. Econ. Geol., 66, 335-341

Guidotti, C. B. (1970) The mineralogy and petrology of the transition from the lower to upper sillimanite zone in the Oquossoc Area, Maine. J. Petrol., 11, 277-336.

Hammarbäck, S. and B. Lindquist (1972) The hydrothermal stability of annite in the presence of sulfur. Geol. Fören. Förh., 94, 549-564.

Harvey, C. S. C. (1975) Petrography, structure and trace element content of wall rock biotites from the Boyd and Calloway ore bodies, Ducktown, Tennessee. M. S. Thesis, North Carolina State University, Raleigh, N. C., 75 p.

Hewitt, D. A. and D. R. Wones (1975) Physical porperties of some synthetic Fe-Mg-Al trioctahedral biotites. Am. Mineral., 60, 854-862.

Holland, H. D. (1959) Some applications of thermochemical data to problems of ore deposits. I. Stability relations among the oxides,

sulfides, sulfates and carbonates of ore and gangue metals. Econ. Geol., 54, 184-233.

Hougen, O. A., K. M. Watson and R. A. Ragatz (1964) Chemical Process Principle Charts, Third Edition, John Wiley and Sons, New York.

Huebner, J. S. (1971) Buffering techniques for hydrostatic systems at elevated pressures. In, G. Ulmer, Ed., Research Techniques for High Pressure and High Temperature. Springer-Verlag, New York. 367 p.

JANAF Thermochemical Tables (1971) Natl. Stand. Ref. Data Service, Nat. Bur. Stand., 37, 1141 p.

Jacobs, D. C. and W. T. Parry (1974) Geochemistry of biotite from the Santa Rita Stock and its associated potassic and phyllic alteration zones, Central Mining District, Grant County, New Mexico (abstr). Econ. Geol., 69, 1181.

Kullerud, G. and H. S. Yoder (1963) Sulfide-silicate relations. Carnegie Inst. Wash. Year Book, 62, 215-218.

_____ and _____ (1964) Sulfide-silicate relations. Carnegie Inst. Wash. Year Book, 63, 218-222.

Moh, G. H., G. Kullerud, O. Kingman and R. Diffenbach (1964) Studies of Ducktown, Tennessee Ores and Country Rocks. Carnegie Inst. Wash. Year Book 63, p. 211-213.

Naldrett, A. J. and G. M. Brown (1968) Reaction between pyrrhotite and enstatite-ferrosilite solid solutions. Carnegie Inst. Wash. Year Book, 66, 427-429.

Popp, R. K., M. C. Gilbert and J. R. Craig (1977) Stability of Fe-Mg amphiboles with respect to sulfur fugacity. Am. Mineral., 62, 13-30.

Putnam, G. W. (1972) Base metal distribution in granitic rocks: data from the Rocky Hill and Lights Creek Stocks, California. Econ. Geol. 67, 511-527.

Rajamani, V. (1976) Distribution of iron, cobalt, and nickel between synthetic sulfide and orthopyroxene at 900°C. Econ. Geol., 71, 795-802.

Robinson, P. and R. J. Tracy (1977) Sulfide-silicate-oxide equilibria in sillimanite-K-feldspar grade pelitic schists, Central Massachusetts (abstr.). EOS, 58, 524.

Rutherford, M. J. (1973) The phase relations of aluminous iron biotites in the system $KAlSi_3O_8$-$KAlSiO_4$-Al_2O_3-Fe-O-H. J. Petrol., 14, 159-180.

Ryzhenko, B. N. and V. P. Volkov (1971) Fugacity coefficients of some gases in a broad range of temperatures and pressures. Geokhimiya, 7, 760-773 [transl. Geochem. Int., 8, 468-481 (1971)].

Shaw, H. R. and D. R. Wones (1964) Fugacity coefficients for hydrogen gas between 0° and 1000°C, for pressures to 3000 atm. Am. J. Sci., 262, 918-929.

Schairer, J. F. and N. L. Bowen (1955) The system K_2O-Al_2O_3-SiO_2. Am. J. Sci., 253, 681-746.

Staten, W. T. (1976) A chemical study of the silicate minerals of the Great Gossan Lead and surrounding rocks in Southwestern Virginia. M. S. Thesis. Virginia Polytechnic Institute and State University, Blacksburg, Va., 109 p.

Toulmin, P. and P. B. Barton (1964) A thermodynamic study of pyrite and pyrrhotite. Geochim. Cosmochim. Acta, 28, 641-671.

Wones, D. R. (1963) Physical properties of synthetic biotites on the join phlogopite-annite. Am. Mineral., 48, 1300-1321.

_____ and H. P. Eugster (1965) Stability of biotite: experiment, theory and application. Am. Mineral., 50, 1228-1272.

Yund, R. A. and H. T. Hall (1969) Hexagonal and monoclinic pyrrhotites, Econ. Geol., 64, 420-423.

The vita has been removed from the scanned document

SULFIDATION OF SYNTHETIC BIOTITES

by

Jonathan L. Tso

(ABSTRACT)

A series of hydrothermal experiments at 2000 bars have been conducted in order to investigate the systematic relation between biotite composition on the join phlogopite-annite and the composition of pyrrhotite. In an attempt to bracket the sulfide-silicate compositional pairs, three layers within a single capsule were used: 1) pyrite + Fe-rich biotite in the top, 2) sanidine + magnetite in the middle, and 3) troilite + Mg-rich biotite in the bottom. At the conclusion of a bracketting run, the biotite in the top was found to have become more Mg-rich and the biotite in the bottom was found to have become more Fe-rich while a pyrrhotite of apparently homogeneous composition was found throughout the capsule.

Five equilibrium determinations at 700°C have been located:

$(N)_{Po}$	$(Fe/(Fe + Mg))_{Bi}$
0.928	0.496
0.936	0.530
0.945	0.541
0.947	0.581
0.950	0.585

The data demonstrate that biotites tend to become more Mg-enriched with increasingly sulfur-rich compositions of pyrrhotite.

This study can be applied to natural systems in which a pyrrhotite-biotite-magnetite-K-spar assemblage is present. Since sulfides have

been observed to re-equilibrate at lower temperatures while the composition of the Fe-Mg silicates still mirror the conditions of metamorphism, silicate compositions can potentially be used as a measure of f_{S_2} and f_{O_2}. From this, one can attempt to calculate the properties of the vapor during the alteration of the silicates and ore genesis.